2018 26th Mediterranean Conference on Control and Automation (MED)
Zadar, Croatia, June 19-22, 2018

Structure and Evolving Fuzzy Models for Prosthetic Hand Myoelectric-based Control Systems*

Radu-Emil Precup, *Senior Member, IEEE*, Teodor-Adrian Teban, Emil M. Petriu, *Fellow, IEEE*, Adriana Albu, and Ion-Cornel Mituletu

***Abstract*—This paper suggests a structure for prosthetic hand myoelectric-based control systems and a set of evolving Takagi-Sugeno-Kang (TSK) fuzzy models to characterize mathematically the finger dynamics of the human hand for the myoelectric control of prosthetic hands. The fuzzy models represent the reference models in myoelectric-based control systems, the model outputs are the flexion percentages that correspond to the midcarpal joint angles, and the model inputs are the myoelectric signals obtained from eight myoelectric sensors. Different numbers of additional model inputs obtained from past inputs and/or outputs are considered. The structure and parameters of the fuzzy models are evolved by an incremental online identification algorithm (IOIA). The evolving TSK fuzzy models for one finger are tested against the experimental data, and a comparison with similar TSK fuzzy models evolved by another IOIA and a neural network model with similar number of parameters is included.**

I. Introduction

As shown in [1] and [2], the development of myoelectric-based control systems for prosthetic hands include several approaches: on-off control, proportional control, direct control, finite state machine control, pattern recognition-based control, posture control, and regression control. All these approaches are considered in the model-based control design framework, which requires accurate models of the human hand. The human hand in such systems is a Multi Input-Multi Output (MIMO) nonlinear dynamical system, with the inputs represented by the myoelectric signals (MESs) viewed as control signals [3], [4], and the outputs represented by finger angles at various joints.

Some popular myoelectric-based control systems for this very interesting application encompass filtering and classification of MESs that make use of artificial intelligence techniques in terms of neural networks (NNs) and fuzzy logic [2], [5]–[12]. Surveys on the use of MESs in rehabilitation and bio-inspired robots are given in [1], [6], [7], [10]. Recent applications of NNs and fuzzy logic are: the NN-based control of robotic hands [5], the prediction of the muscle force using wavelet NNs [8], the prediction of handgrip force from MESs by extreme learning machines [9], the classification of MESs by NN tree combined with the maximal Lyapunov exponent [11], nonlinear autoregressive with exogenous inputs (NARX) recurrent dynamic NNs and evolving Takagi-Sugeno-Kang (TSK) fuzzy models using MESs obtained from five myoelectric sensors (MSs) placed on human subject's arm [2], [12]. Real-world examples of myoelectric-based control systems of prosthetic arms are described in [13]–[15].

The concept of evolving fuzzy (rule-based) controllers was coined by P. Angelov back in 2001 and further developed in his later works [16]–[21]. These controllers are related to evolving TSK fuzzy models, for which the rule bases are computed by a learning process, namely continuous online rule base learning as shown in the recent papers [22]–[26]. However, learning can next also be related to control. With this regard, constructing virtual state-space process models from input-output (I/O) data samples can be carried out. Then, reinforcement learning (eventually with NN or TSK fuzzy models) can be used to learn the controllers for this virtual process, requiring theoretical developments to prove that the virtual processes are fully state observable and their control is equivalent to I/O control of the initial process.

This paper is a sequel to our previously published papers on prosthetics [2], [12], [27], evolving TSK fuzzy models [2], [22], [25], nonlinear NARX recurrent dynamic NN models [12]. This paper suggests a structure for prosthetic hand myoelectric-based control systems and a set of evolving TSK fuzzy models of the human hand dynamics, i.e., the finger dynamics to be used as reference models in myoelectric-based control systems. The inputs of this nonlinear system are the MESs obtained from eight sensors placed on human subject's arm, and the outputs are the flexion percentages that correspond to the midcarpal joint angles. The flexion percentages are also called finger angles for simplicity.

Particularly, the structure concept in the paper title requires clarification. This structure is related to the control system structure for prosthetic hand myoelectric-based control. This structure is not the rule-base structure, it is given as a general architecture in the next section, and it is different from other applications by the hierarchical architecture suggested here. This has not been addressed so far with other process models including the same fuzzy identification algorithm and other controllers as well. Combined with the new TSK fuzzy models, this represents the amount of novelty which could be assessed as significant.

*Research supported by Accenture and the NSERC of Canada.

R.-E. Precup, T.-A. Teban, A. Albu, and I.-C. Mituletu are with the Department of Automation and Applied Informatics, Politehnica University of Timisoara, Bd. V. Parvan 2, 300223 Timisoara, Romania (phone: +40 256403229, fax: +40 256403214; e-mail: radu.precup@upt.ro, adrian.teban@student.upt.ro, adriana.albu@upt.ro, ion.mituletu@student.upt.ro). I.-C. Mituletu is also with the Department of Electrical and Computer Engineering, "Eftimie Murgu" University of Resita, P-ta Traian Vuia 1-4, 320085 Resita, Romania.

E. M. Petriu is with the School of Electrical Engineering and Computer Science, University of Ottawa, Ottawa, ON K1N 6N5, Canada (e-mail: petriu@uottawa.ca).

The paper does not contain important details on the experimental setup used (i.e., what sensors have been used, what sensitivity, frequency band, electrodes, etc.) as it is mainly focused on modeling. However, these details would lead to a substantially higher technical content of the experimental part of the paper.

This paper is organized as follows: the myoelectric-based control system structure is described in the next section. The main implementation details of the incremental online identification algorithm (IOIA) are given in Section III. Aspects concerning the development of evolving TSK fuzzy models and experimental results related to the models of the first finger are presented in Section IV. A performance comparison with the TSK fuzzy models evolved by DENFIS [28], which is another IOIA, and an NN model (a NARX one) with similar number of parameters is carried out; the root mean square error (RMSE) values illustrate the superiority of the TSK fuzzy models suggested in this paper. The conclusions are highlighted in Section V.

II. Myoelectric-based Control System Structure

The system aim is to replicate a real human hand operation based on the electric signals going to the muscles. The myoelectric-based control system architecture presented in Fig. 1 is proposed to be employed with this regard.

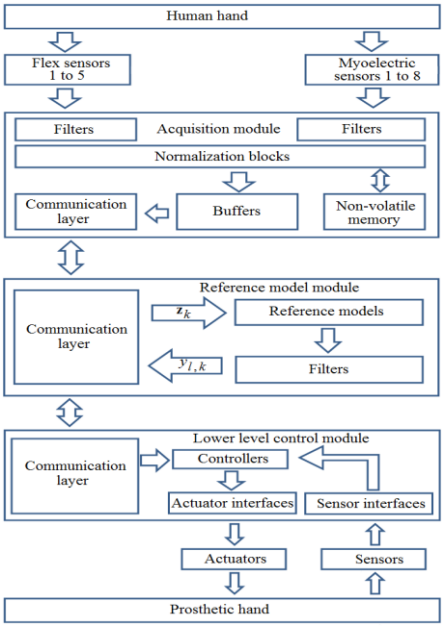

Fig. 1. Myoelectric-based control system architecture.

The system makes use of eight MSs, which capture the electrical signals, i.e., the MESs. The MSs are connected to the muscles in a non-invasive way, and send the MESs to the reference model for processing. Five flex sensors are employed, which measure the finger angles for training and validating the reference models.

The myoelectric-based control system consists of three independent subsystems referred to also as modules: sensor acquisition, reference model, and lower level control. This splitting is done because the modular subsystems can be treated as black boxes, and their inputs and outputs can be easily monitored. The main module of the architecture proposed in his paper is the reference model one, which can output undesired values especially for untrained data and must be isolated from the rest of the system. The system can also be easier designed and trained if the reference models are devoted only to processing the correlation between MESs and desired finger angles without focusing on lower level control or filtering.

The three subsystems presented in Fig. 1 are briefly described as follows. *The sensor acquisition module* is built around the following hardware configuration, with additional details presented in [2]: microcontroller-based system in order to ensure real-time acquisition, flex sensor board to transform flex sensor resistances into voltages, and myoelectric board to amplify, rectify and filter the muscle voltages. This module acquires the input data from the myoelectric and flex sensors at the sampling period $T_s = 0.01$ s, filters the measured values, calculates and saves (in non-volatile memory) the range of the signals from MESs and flex sensors for hand fully closed and fully opened (done only in training mode) and normalizes the new values of all sensors so they will be in the same range. The normalized values are stored into a buffer used for filtering the output of the module using a weighted average between the current value (70%) and the previous value (30%) then sends flex and myoelectric measured values through Universal Asynchronous Receiver/Transmitter (UART) for processing.

The reference model module consists of a communication module that receives measured values from the acquisition module, requests recalibration to the acquisition module if the sensor positions are slightly changed, and sends the reference inputs expressed as desired (or imposed) flexion percentages (finger angles) to the lower level control module. The reference models are nonlinear; fuzzy models are developed in this paper. The output of the module is passed through an average weight filter (three past values), in order to smooth out the sudden spikes of the fuzzy model, before being sent to the communication interface.

All reference models (TSK fuzzy ones and NNs to be next treated) use the same eight inputs that belong to the vector

$$[z_{1,k} \;\; z_{2,k} \;\; z_{3,k} \;\; z_{4,k} \;\; z_{5,k} \;\; z_{6,k} \;\; z_{7,k} \;\; z_{8,k}]^T, \quad (1)$$

where the superscript T indicates matrix transposition, k is the index of the current sample, $z_{j,k}$ (b), 0 b $\le z_{j,k} \le$ 255 b, is the MES obtained as the output of the MS j, $j = 1...8$, and the measuring unit b stands for bit. The placement of four out of the eight MSs on the human hand is shown in Fig. 2.

The input vector in (1) makes use of information from all MSs because of the need to model the effects of cross-couplings in the MIMO nonlinear dynamical system represented by the human hand. The dynamics is inserted in the models by means of several past values of the outputs and/or inputs by appropriate shifting and not measuring.

The outputs of all reference models are the finger angles $y_{l,k}$ (%) of the fingers l, $l = 1...5$, expressed as flexion percentages that correspond to the midcarpal joint angles

between fully relaxed (0) and fully contracted (100), $0\,\% \le y_{l,k} \le 100\,\%$. The finger indices l are $l=1$ for the thumb, $l=2$ for the index finger, $l=3$ for the middle finger, $l=4$ for the ring finger, and $l=5$ for the pinky.

Fig. 2. Placement of myoelectric sensors 1, 2, 3 and 4 on the human hand.

The lower level control module receives angle reference inputs from the reference model module, manages the information from sensors (force, angle) and implements the controllers that elaborate the control signals applied to the actuators (servos). This module is referred to as lower level because the coordination and computation of reference inputs can be conducted at higher hierarchical levels, and the communication layer enables the information transfer between the control levels in both directions.

III. Online Identification Algorithm

The IOIA is implemented using the theory adapted from [29] and supported by the eFS Lab software described in [30]. The flowchart of IOIA is presented in Fig. 3. This algorithm is organized in terms of the following steps, namely S1 – S7, also described in [2] and [22]:

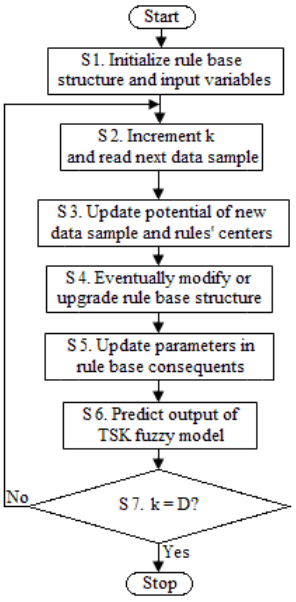

Fig. 3. Flowchart of incremental online identification algorithm.

S1. The rule base structure is initialized. All parameters in the rule antecedents are set to obtain one rule, $n_R = 1$ (n_R – the number of rules). The parameters of the evolving TSK fuzzy models using are calculated by subtractive clustering for the first data point $\mathbf{p}_1$. The notation $\mathbf{p}_k$ is employed for the data point $\mathbf{p}$ at the discrete time step k (that is also the index of the current sample), which belongs to the I/O data set $\{\mathbf{p}_k \mid k = 1...D\} \subset \Re^{n+1}$

$$\mathbf{p}_k = [p_k^1 \;\; p_k^2 \ldots p_k^{n+1}]^T,\; \mathbf{p} = [\mathbf{z}^T \;\; y]^T = [z_1 \;\; z_2 \ldots z_n \;\; y_l]^T = [p^1 \;\; p^2 \ldots p^n \;\; p^{n+1}]^T \in \Re^{n+1}, \tag{2}$$

where D is the number of I/O data points or data samples, and $\mathbf{z}$ is the input vector.

The rule base of TSK fuzzy models, considered here in the particular case that involves affine rule consequents, is

$$\begin{aligned} &\text{Rule} \;\; i: \text{IF } z_1 \text{ IS } LT_{i1} \text{ AND } \ldots \text{ AND } z_n \text{ IS } LT_{in} \\ &\text{THEN } y_l^i = a_{i0} + a_{i1} z_1 + \ldots + a_{in} z_n, i = 1...n_R, \end{aligned} \tag{3}$$

where $z_j,\; j = 1...n,$ are the input (or scheduling) variables, n is the number of input variables, $LT_{ij}, i = 1...n_R, j = 1...n,$ are the input linguistic terms, y_l^i is the output of the local model in the rule consequent of rule $i, i = 1...n_R,$ and $a_{i\chi}, i = 1...n_R,$ $\chi = 0...n,$ are the parameters in the rule consequents.

Considering the algebraic product t-norm as an AND operator and the weighted average defuzzification method, the expression of the TSK fuzzy model output y_l is

$$\begin{aligned} &y_l = [\sum_{i=1}^{n_R} \tau_i y_l^i] / [\sum_{i=1}^{n_R} \tau_i] = \sum_{i=1}^{n_R} \lambda_i y_l^i,\;\; y_l^i = [1 \;\; \mathbf{z}^T] \boldsymbol{\pi}_i, \\ &\lambda_i = \tau_i / [\sum_{i=1}^{n_R} \tau_i],\;\; i = 1...n_R, \end{aligned} \tag{4}$$

where the $\tau_i(\mathbf{z})$ is firing degree of rule i and $\lambda_i(\mathbf{z})$ the normalized firing degree, and the parameter vector of rule i is $\boldsymbol{\pi}_i, i = 1...n_R$, $\tau_i(\mathbf{z})$ is calculated in terms of

$$\begin{aligned} \tau_i(\mathbf{z}) &= \text{AND}\,(\mu_{i1}(z_1), \mu_{i2}(z_2), ..., \mu_{in}(z_n)) \\ &= \mu_{i1}(z_1) \cdot \mu_{i2}(z_2) \cdot \ldots \cdot \mu_{in}(z_n),\;\; i = 1...n_R, \end{aligned} \tag{5}$$

and the parameter vector of rule i is $\boldsymbol{\pi}_i$

$$\boldsymbol{\pi}_i = [a_{i0} \;\; a_{i1} \;\; a_{i2} \;\; \ldots \;\; a_{in}]^T, i = 1...n_R. \tag{6}$$

Some parameters specific to IOIA are initialized as [29]

$$\begin{aligned} &\hat{\boldsymbol{\theta}}_1 = [(\boldsymbol{\pi}_1^T)_1 \;\; (\boldsymbol{\pi}_2^T)_1 \ldots (\boldsymbol{\pi}_{n_R}^T)_1]^T = [0 \;\; 0 \ldots 0]^T, \\ &\mathbf{C}_1 = \Omega\, \mathbf{I},\;\; r_s = 0.4,\;\; k = 1,\;\; n_R = 1,\;\; \mathbf{z}_1^* = \mathbf{z}_k,\;\; P_1(\mathbf{p}_1^*) = 1, \end{aligned} \tag{7}$$

where $\mathbf{C}_k \in \Re^{n_R(n+1) \times n_R(n+1)}$ is the fuzzy covariance matrix (clusters), $\mathbf{I}$ is the $n_R(n+1)^{\text{th}}$ order identity matrix, $\Omega = \text{const}, \Omega > 0,$ is a large number, $\hat{\boldsymbol{\theta}}_k$ is an estimation of the parameter vector in the rule consequents at time k, and $r_s,\; r_s > 0,$ is the spread of all Gaussian input membership functions (m.f.s) $\mu_{ij}, i = 1...n_R, j = 1...n,$ of the fuzzy sets afferent to the input linguistic terms LT_{ij}

$$\mu_{ij}(z_j) = \exp[-4(z_j - z_{ij}^*)^2 / r_s^2],\;\; i = 1...n_R,\;\; j = 1...n, \tag{8}$$

$z_{ij}^*\;\; i = 1...n_R, j = 1...n,$, are the m.f. centers, $\mathbf{p}_1^*$ in (8) is the first cluster center, $\mathbf{z}_1^*$ is the center of rule 1, equal to the projection of $\mathbf{p}_1^*$ on the axis $\mathbf{z}$ in terms of (2), and $P_1(\mathbf{p}_1^*)$ is the potential of $\mathbf{p}_1^*$.

S2. The data sample index k is incremented, and the next data sample $\mathbf{p}_k$ that belongs to the I/O data set $\{\mathbf{p}_k \mid k = 1...D\} \subset \Re^{n+1}$ is collected.

S3. The potential of each new data sample $P_k(\mathbf{p}_k)$ and the potentials of the centers $P_k(\mathbf{p}_\eta^*)$ of existing rules (clusters) with the index η are recursively updated.

S4. If certain conditions [29] are fulfilled, the rule base structure is modified or upgraded using potential of the new data in comparison with that of the existing rules' centers.

S5. The parameters in the rule consequents are updated using either the Recursive Least Squares (RLS) algorithm with a global objective function or the weighted Recursive Least Squares (wRLS) algorithm with a locally weighted objective function. These updates allow for the computation of the updated $\hat{\boldsymbol{\theta}}_k$ and $\mathbf{C}_k$, $k = 2...D$.

S6. The output of the evolving TSK fuzzy model at the next discrete time step *k*+1 is predicted:

$$\hat{y}_{k+1} = \boldsymbol{\psi}_k^T \hat{\boldsymbol{\theta}}_k, \tag{9}$$

with the notations

$$\begin{aligned} &y = \boldsymbol{\psi}^T \boldsymbol{\theta},\ \boldsymbol{\theta} = [\boldsymbol{\pi}_1^T \quad \boldsymbol{\pi}_2^T \quad ... \quad \boldsymbol{\pi}_{n_R}^T]^T, \\ &\boldsymbol{\psi}^T = [\lambda_1[1 \ \mathbf{z}^T] \quad \lambda_2[1 \ \mathbf{z}^T] \quad ... \quad \lambda_{n_R}[1 \ \mathbf{z}^T]]. \end{aligned} \tag{10}$$

S7. The algorithm continues with S2 until all data points of the I/O data set $\{\mathbf{p}_k \mid k = 1...D\}$ are collected.

As suggested in [22], RLS and wRLS in S5 can be replaced with other optimization algorithms. Classical and metahauristic algorithms can be inserted in optimization problems in various applications as large-scale [31], robotics [32]–[35], medical [36], [37], and servo systems [38], [39].

IV. Fuzzy Models and Experimental Results

The IOIA presented in the previous section was applied to get evolving TSK fuzzy models of the finger dynamics. Some results for the thumb (the first finger, $l = 1$) and implementation details are presented as follows. The value $\Omega = 10000$ vas set in S1.

As pointed out in Section I, the dynamics is inserted in TSK fuzzy models by means of several past values of the output (the finger angle) $y_{1,k}$, computed by shifting and not measured. This leads to the nonlinear I/O map f, which enables to consider the TSK fuzzy models $y_{1,k} = f(\mathbf{z}_k)$ as NARX models.

The rule consequents parameters are updated in S5 using either RLS or wRLS. This leads to 27 TSK fuzzy models with the inputs specified in Table I, which includes the TSK fuzzy models evolved by DENFIS.

The paper struggles with the problem of clash between the order of system dynamics introduced into the evolution of fuzzy models and the computational complexity that grows with the model order. The TSK fuzzy models evolved by IOIA were compared with a recurrent NN model that implements the NARX model $y_{1,k} = f(\mathbf{z}_k)$. The TSK fuzzy models evolved by DENFIS were derived to obtain the maximum number of rules that is close to that obtained by the algorithm given in Section III for the same input vectors. The parameter settings specific to DENFIS were set to their default values given in [28]–[31]. The architecture of the NN is given in [12] for five instead of eight elements of the vector in (1), and the relation of the recurrent NN with the TSK fuzzy models is that they are nonlinear models, which operate with the same inputs and approximately the same number of parameters that are identified.

TABLE I. Input Vectors and Optimization Algorithms in Rule Consequents Parameters Computation (M.n. – Model Number)

M.n.	Input vector $\mathbf{z}_k$ and optimization algorithm
1/2/3	$\mathbf{z}_k = [z_{1,k} \ z_{2,k} \ z_{3,k} \ z_{4,k} \ z_{5,k} \ z_{6,k} \ z_{7,k} \ z_{8,k}]^T$, RLS/wRLS/D ENFIS
4/5/6	$\mathbf{z}_k = [z_{1,k} \ z_{2,k} \ z_{3,k} \ z_{4,k} \ z_{5,k} \ z_{6,k} \ z_{7,k} \ z_{8,k} \ y_{1,k-1}]^T$, RLS/wRLS/D ENFIS
7/8/9	$\mathbf{z}_k = [z_{1,k} \ z_{2,k} \ z_{3,k} \ z_{4,k} \ z_{5,k} \ z_{6,k} \ z_{7,k} \ z_{8,k}$ $y_{1,k-1} \ y_{2,k-1} \ y_{3,k-1} \ y_{4,k-1} \ y_{5,k-1}]^T$, RLS/wRLS/D ENFIS
10/11/12	$\mathbf{z}_k = [z_{1,k} \ z_{2,k} \ z_{3,k} \ z_{4,k} \ z_{5,k} \ z_{6,k} \ z_{7,k} \ z_{8,k} \ y_{1,k-1} \ y_{1,k-2}]^T$, RLS/wRLS/D ENFIS
13/14/15	$\mathbf{z}_k = [z_{1,k} \ z_{2,k} \ z_{3,k} \ z_{4,k} \ z_{5,k} \ z_{6,k} \ z_{7,k} \ z_{8,k} \ y_{1,k-1}$ $y_{2,k-1} \ y_{3,k-1} \ y_{4,k-1} \ y_{5,k-1} \ y_{1,k-2}]^T$, RLS/wRLS/D ENFIS
16/17/18	$\mathbf{z}_k = [z_{1,k} \ z_{2,k} \ z_{3,k} \ z_{4,k} \ z_{5,k} \ z_{6,k} \ z_{7,k} \ z_{8,k} \ z_{1,k-1} \ z_{2,k-1}$ $z_{3,k-1} \ z_{4,k-1} \ z_{5,k-1} \ z_{6,k-1} \ z_{7,k-1} \ z_{8,k-1} \ y_{1,k-1}]^T$, RLS/wRLS/D ENFIS
19/20/21	$\mathbf{z}_k = [z_{1,k} \ z_{2,k} \ z_{3,k} \ z_{4,k} \ z_{5,k} \ z_{6,k} \ z_{7,k} \ z_{8,k} \ z_{1,k-1} \ z_{2,k-1}$ $z_{3,k-1} \ z_{4,k-1} \ z_{5,k-1} \ z_{6,k-1} \ z_{7,k-1} \ z_{8,k-1} \ y_{1,k-1} \ y_{2,k-1}$ $y_{3,k-1} \ y_{4,k-1} \ y_{5,k-1}]^T$, RLS/wRLS/D ENFIS
22/23/24	$\mathbf{z}_k = [z_{1,k} \ z_{2,k} \ z_{3,k} \ z_{4,k} \ z_{5,k} \ z_{6,k} \ z_{7,k} \ z_{8,k} \ z_{1,k-1} \ z_{2,k-1}$ $z_{3,k-1} \ z_{4,k-1} \ z_{5,k-1} \ z_{6,k-1} \ z_{7,k-1} \ z_{8,k-1} \ y_{1,k-1} \ y_{1,k-2}]^T$, RLS/wRLS/D ENFIS
25/26/27	$\mathbf{z}_k = [z_{1,k} \ z_{2,k} \ z_{3,k} \ z_{4,k} \ z_{5,k} \ z_{6,k} \ z_{7,k} \ z_{8,k} \ z_{1,k-1} \ z_{2,k-1}$ $z_{3,k-1} \ z_{4,k-1} \ z_{5,k-1} \ z_{6,k-1} \ z_{7,k-1} \ z_{8,k-1} \ y_{1,k-1} \ y_{2,k-1}$ $y_{3,k-1} \ y_{4,k-1} \ y_{5,k-1} \ y_{1,k-2}]^T$, RLS/wRLS/D ENFIS

The eight system inputs were generated to capture various hand movements on a long time horizon of 434.91 s, namely 250 s for training plus 184.91 s for validation. The outputs were measured. The time evolution of the system inputs is presented in Fig. 4, which includes the input data for training and validation.

Much information is shown in the graphs and no clear thing can be extracted, but the idea is to show the nature of the input values (given here for three ones out of all). This noisy nature of the signals is similar in all inputs.

Fig. 4 illustrates the inputs both the $D = 25000$ training data points and the $D = 18491$ validation data points. The real system output values will be presented along with the model outputs.

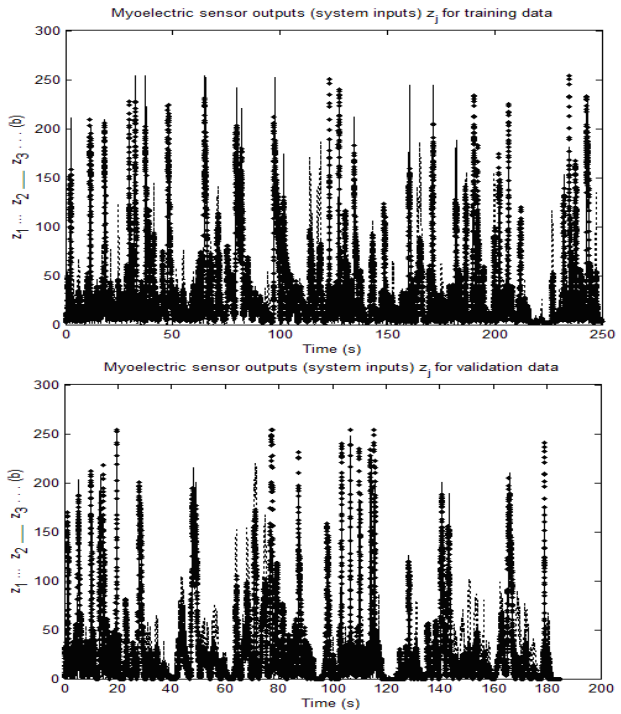

Fig. 4. System inputs $z_{1,k}$, $z_{2,k}$ and $z_{3,k}$ versus time for training and validation data.

The number of parameters and rules of the final evolved TSK fuzzy models and the recurrent NN model are presented in Table II for the best first finger angle models. The values of the RMSE between the model outputs $y_{1,k}$ and the real-world system outputs (the human hand finger angles) $y_{d1,k}$ (the expected outputs) are also included in Table II, which includes results for training and validation. The RMSE, as a global performance index, is calculated in terms of

$$\text{RMSE} = \sqrt{(1/D)\sum_{k=1}^{D}(y_{1,k} - y_{d1,k})^2}, \qquad (11)$$

where the real-world system outputs $y_{d1,k}$ were obtained by real-time measurements conducted on the human hand.

TABLE II. NUMBERS OF PARAMETERS (N.P.), NUMBERS OF RULES AND RMSE ON TRAINING AND VALIDATION DATA CONCERNING THE MODELS DEVELOPED FOR THE FIRST FINGER

M.n.	N.p.	n_R	RMSE training	RMSE validation
10	310	10	1.0931	1.0978
13	817	19	1.0198	1.0635
22	550	10	1.0515	1.0872
25	1273	19	1.0016	1.0583
26	1273	19	1.0332	1.0662
NN	328	-	1.3724	1.3722

The Levenberg-Marquardt algorithm was applied to train the NARX recurrent NN model. The stopping criterion is reaching an imposed upper absolute modeling error. Overfitting or underfitting can decrease the NN performance. More details about the recurrent NN model are not provided as we focus on fuzzy modeling and next fuzzy control.

The TSK fuzzy models and their performance depend on the number of input variables. Different model structures are obtained for other input variables.

Table II indicates that the validation performance is consistent with the training one in terms of RMSE. The TSK fuzzy models exhibit better performance versus the NN with similar complexity (i.e., number of parameters trained) considered here. There are no measurable results that support this statement except the numbers appearing in the last row; the importance of this comparison is not emphasized as the performance enhancement is clearly visible. Our TSK fuzzy models ensure the global performance improvement versus the TSK fuzzy models with similar complexity (the same row in Table I) evolved by DENFIS.

The comparison in section IV is not presented in more detail in order to keep a balance between the structure, the algorithm and the validation. A part of the real-time experimental results on the validation data set is exemplified in Fig. 5 for the TSK fuzzy model 10.

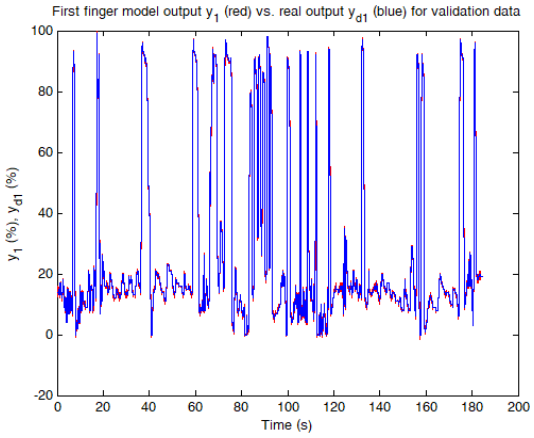

Fig. 5. Flex percentage (finger angle) y_1 versus time of TSK fuzzy model 10 (red) and of real-world system (blue) on the validation data set.

Increasing the number of input variables with more past (delayed) system inputs and/or outputs with respect to the currently considered ones can lead to fuzzy model performance improvement. However, this model improvement solution should be treated with great attention as the number of parameters will increase, also resulting in increased training time and decreased generalization capability. As shown in [2], a regression test can be performed to reduce the bias-variance tradeoff, an alternative being Akaike information criterion.

V. CONCLUSION

This paper has suggested a structure for prosthetic hand myoelectric-based control systems and a set of TSK fuzzy models to model the finger angles. The structure and parameters of the TSK fuzzy models have been obtained by an incremental online identification algorithm.

The models have been tested with approximately 450 s, but more people and larger data sets could conclude in different results. Actually, the results indicate that past samples of the output have increased the performance of the model significantly, so that one or two extra past samples

increase the performance even more without increasing the number of parameters. Nevertheless, the number of parameters depends on the identification algorithm.

Future research will target the development of more efficient fuzzy models of this nonlinear dynamic subsystem that belongs to myoelectric-based control systems to give cost-effective models (small numbers of parameters and computation time). Experiments will be conducted on test data to check the performance of the chosen models in unseen data corresponding to different hand movements.

REFERENCES

[1] P. Geethanjali, "Myoelectric control of prosthetic hands: state-of-the-art review," *Med. Dev. Evid. Res.*, vol. 9, pp. 247–255, Dec. 2016.

[2] R.-E. Precup, T.-A. Teban, T. E. Alves de Oliveira, and E. M. Petriu, "Evolving fuzzy models for myoelectric-based control of a prosthetic hand," in *Proc. 2016 IEEE Intl. Conf. Fuzzy Syst.*, Vancouver, BC, Canada, 2016, pp. 72–77.

[3] M. Borghetti, E. Sardini, and M. Serpelloni, "Sensorized glove for measuring hand finger flexion for rehabilitation purposes," *IEEE Trans. Instrum. Meas.*, vol. 62, no. 12, pp. 3308–3314, Dec. 2013.

[4] Z. Ma, P. Ben-Tzvi, and J. Danoff, "Hand rehabilitation learning system with an exoskeleton robotic glove," *IEEE Trans. Neural Syst. Rehabil. Eng.*, vol. 24, no. 12, pp. 1323–1332, Dec. 2016.

[5] J.-H. Wang, H.-C. Ren, W.-H. Chen, and P. Zhang, "A portable artificial robotic hand controlled by EMG signal using ANN classifier," in *Proc. 2015 IEEE Intl. Conf. Inform. Autom.*, Lijiang, China, 2015, pp. 2709–2714.

[6] E. J. Rechy-Ramirez and H.-S. Hu, "Bio-signal based control in assistive robots: a survey," *Dig. Commun. Netw.*, vol. 1, no. 2, pp. 85–101, Apr. 2015.

[7] M. S. H. Bhuiyan, I. A. Choudhury, and M. Dahari, "Development of a control system for artificially rehabilitated limbs: a review," *Biol. Cybern.*, vol. 109, no. 2, pp. 141–162, Apr. 2015.

[8] Z.-J. Xu, Y.-T. Tian, and L. Yang, "sEMG pattern recognition of muscle force of upper arm for intelligent bionic limb control," *J. Bionic Eng.*, vol. 12, no. 2, pp. 316–323, Apr. 2015.

[9] H.-X. Cao, S.-Q. Sun, and K.-J. Zhang, "Modified EMG-based handgrip force prediction using extreme learning machine," *Soft Comput.*, vol. 21, no. 2, pp. 491–500, Jan. 2017.

[10] W. Meng, Q. Liu, Z. Zhou, Q.-S. Ai, B. Sheng, and S.-Q. Xie, "Recent development of mechanisms and control strategies for robot-assisted lower limb rehabilitation," *Mechatronics*, vol. 31, pp. 132–145, Oct. 2015.

[11] Y. Guo, G. R. Naik, S. Huang, A. Abraham, and H. T. Nguyen, "Nonlinear multiscale maximal Lyapunov exponent for accurate myoelectric signal classification," *Appl. Soft Comput*., vol. 36, pp. 633–640, Nov. 2015.

[12] T.-A. Teban, R.-E. Precup, T. E. Alves de Oliveira, and E. M. Petriu, "Recurrent dynamic neural network model for myoelectric-based control of a prosthetic hand," in *Proc. 2016 IEEE Intl. Syst. Conf.*, Orlando, FL, USA, 2016, pp. 1–6.

[13] DARPA, "Proto 2," *Popular Sci. Mag.*, Aug. 2007.

[14] Advanced Arm Dynamics, "Philly, welcome to the bionic age," *Metro*, July 2011.

[15] Advanced Arm Dynamics, "Advanced surgery helps 13-year-old move prosthetic arm," *CBS Minnesota*, Sep. 2015.

[16] P. Angelov, R. A. Buswell, J. A. Wright, and D. L. Loveday, "Evolving rules-based control," in *Proc. EUNITE 2001 Symp.*, Tenerife, Spain, 2001, pp. 36–41.

[17] P. Angelov and R.A. Buswell, "Identification of evolving fuzzy rule-based models," *IEEE Trans. Fuzzy Syst.*, vol. 10, no. 5, pp. 667–677, Oct. 2002.

[18] P. Angelov, *Evolving Rule-Based Models: A Tool for Design of Flexible Adaptive Systems*. Heidelberg: Springer-Verlag, 2002.

[19] P. Angelov and D. Filev, "Flexible models with evolving structure," in *Proc. 2002 First Intl. IEEE Symp. Intell. Syst.*, Varna, Bulgaria, 2002, pp. 28–33.

[20] P. Angelov and D. Filev, "On-line design of Takagi-Sugeno models," in *Fuzzy Sets and Systems - IFSA 2003*, T. Bilgiç, B. De Baets, and O. Kaynak, Eds. Berlin, Heidelberg: Springer-Verlag, Lect. Notes Comput. Sci., vol. 2715, pp. 576–584, 2003.

[21] P. Sadeghi-Tehran, A. B. Cara, P. Angelov, H. Pomares, I. Rojas, and A. Prieto, "Self-evolving parameter-free rule-based controller," in *Proc. 2012 World Congr. Comput. Intell.*, Brisbane, Australia, 2012, pp. 754–761.

[22] P. Angelov, I. Škrjanc, and S. Blažič, "Robust evolving cloud-based controller for a hydraulic plant," in *Proc. 2013 IEEE Conf. Evolv. Adapt. Syst.*, Singapore, 2013, pp. 1–8.

[23] S. Blažič, I. Škrjanc, and D. Matko, "A robust fuzzy adaptive law for evolving control systems," *Evolv. Syst.*, vol. 5, no. 1, pp. 3–10, Mar. 2014.

[24] R.-E. Precup, H.-I. Filip, M.-B. Radac, E. M. Petriu, S. Preitl, and C.-A. Dragos, "Online identification of evolving Takagi-Sugeno-Kang fuzzy models for crane systems," *Appl. Soft Comput.*, vol. 24, pp. 1155–1163, Nov. 2014.

[25] D. Leite, R. M. Palhares, V. C. S. Campos, and F. A. C. Gomide, "Evolving granular fuzzy model-based control of nonlinear dynamic systems," *IEEE Trans. Fuzzy Syst.*, vol. 23, no. 4, pp. 923–938, Aug. 2015.

[26] R.-E. Precup, P. Angelov, B. S. J. Costa, and M. Sayed-Mouchaweh, "An overview on fault diagnosis and nature-inspired optimal control of industrial process applications," *Comput. Ind.*, vol. 74, pp. 75–94, Dec. 2015.

[27] P. Wide, E. M. Petriu, and M. Siegel, "Sensing and perception for rehabilitation and enhancement of human natural capabilities," in *Proc. 2010 IEEE Int. Workshop Robotic Sens. Env.*, Phoenix, AZ, USA, 2010, pp. 75–80.

[28] N. Kasabov, "ECOS: A framework for evolving connectionist systems and the eco learning paradigm," in *Proc. 5th Intl. Conf. Neural Inf. Proc.*, Kitakyushu, Japan, 1998, pp. 1222–1235.

[29] P. Angelov and D. Filev, "An approach to online identification of Takagi-Sugeno fuzzy models," *IEEE Trans. Syst., Man, Cybern. B, Cybern.*, vol. 34, no. 1, pp. 484–498, Feb. 2004.

[30] J. V. Ramos and A. Dourado, "On line interpretability by rule base simplification and reduction," in *Proc. Eur. Symp. Intell. Technol. Hybrid Syst. Their Implem. Smart Adapt. Syst.*, Aachen, Germany, 2004, pp. 1–6.

[31] F. G. Filip, "Decision support and control for large-scale complex systems," *Ann. Rev. Control*, vol. 32, no. 1, pp. 61–70, Apr. 2008.

[32] A. Vasilijević, B. Borović, and Z. Vukić, "Underwater vehicle localization with complementary filter: performance analysis in the shallow water environment," *J. Intell. Robot. Syst.*, vol. 68, no. 3–4, pp. 373 – 386, Dec. 2012.

[33] N. Smolić-Ročak, S. Bogdan, Z. Kovačić, and T. Petrović, "Time windows based dynamic routing in multi-AGV systems," *IEEE Trans. Autom. Sci. Eng.*, vol. 7, no. 1, pp. 151–155, Jan. 2010.

[34] J. Vaščák and K. Hirota, "Integrated decision-making system for robot soccer," *J. Adv. Comput. Intell. Intell. Informat.*, vol. 15, no. 2, pp. 156–163, Mar. 2011.

[35] K. Michail, K. M. Deliparaschos, S. G. Tzafestas, and A. C. Zolotas, "AI-based actuator/sensor fault detection with low computational cost for industrial applications," *IEEE Trans. Control Syst. Technol.*, vol. 24, no. 1, pp. 293–301, Jan. 2016.

[36] A. Sánchez Boza, R. H. Guerra, and A. Gajate, "Artificial cognitive control system based on the shared circuits model of sociocognitive capacities. A first approach," *Eng. Appl. Artif. Intell*., vol. 24, no. 2, pp. 209–219, Mar. 2011.

[37] L. Kovács, "Linear parameter varying (LPV) based robust control of type-I diabetes driven for real patient data," Knowl.-Based Syst., vol. 122, pp. 199–213, Apr. 2017.

[38] R.-E. Precup, R.-C. David, and E. M. Petriu, "Grey wolf optimizer algorithm-based tuning of fuzzy control systems with reduced parametric sensitivity," *IEEE Trans. Ind. Electron.*, vol. 64, no. 1, pp. 527–534, Jan. 2017.

[39] M. P. R. Reddy, and J. Jacob, "Vibration control of flexible link manipulator using SDRE controller and Kalman filtering," S*tud. Informat. Control*, vol. 26, no. 2, pp. 143–150, Jun. 2017.